Ultrasonics Sonochemistry 92 (2023) 106241

Contents lists available at ScienceDirect

Ultrasonics Sonochemistry

journal homepage: www.elsevier.com/locate/ultson

Ultrasonic-assisted synthesis of lignin-capped Cu_2O nanocomposite with antibiofilm properties

Moorthy Maruthapandi [a,b,1], Akanksha Gupta [a,b,1], Arumugam Saravanan [a,b], Gila Jacobi [c], Ehud Banin [c], John H.T. Luong [d], Aharon Gedanken [a,b,*]

[a] Bar-Ilan Institute for Nanotechnology and Advanced Materials (BINA), Bar-Ilan University, Ramat-Gan 5290002, Israel
[b] Department of Chemistry, Bar-Ilan University, Ramat-Gan 5290002, Israel
[c] The Mina and Everard Goodman Faculty of Life Sciences, Institute for Nanotechnology and Advanced Materials, Bar-Ilan University, Ramat-Gan 52900, Israel
[d] School of Chemistry, University College Cork, Cork T12 YN60, Ireland

ARTICLE INFO

Keywords:
Ultrasonic method
Lignin Cu_2O nanocomposite
Cytotoxicity
Antimicrobial
Antibiofilm

ABSTRACT

Under ultrasonication, cuprous oxide (Cu_2O) microparticles (<5 μm) were fragmented into nanoparticles (NPs, ranging from 10 to 30 nm in diameter), and interacted strongly with alkali lignin (Mw = 10 kDa) to form a nanocomposite. The ultrasonic wave generates strong binding interaction between lignin and Cu_2O. The L-Cu nanocomposite exhibited synergistic effects with enhanced antibiofilm activities against *E. coli*, multidrug-resistant (MDR) *E. coli*, *S. aureus* (SA), methicillin-resistant SA, and *P. aeruginosa* (PA). The lignin-Cu_2O (L-Cu) nanocomposite also imparted notable eradication of such bacterial biofilms. Experimental evidence unraveled the destruction of bacterial cell walls by L-Cu, which interacted strongly with the bacterial membrane. After exposure to L-Cu, the bacterial cells lost the integrated structural morphology. The estimated MIC for biofilm inhibition for the five tested pathogens was 1 mg/mL L-Cu (92 % lignin and 8 % Cu_2ONPs, w/w %). The MIC for bacterial eradication was noticeably lower; 0.3 mg/mL (87 % lignin + 13 % Cu_2ONPs, w/w %) for PA and SA, whereas this value was appreciably higher for MDR *E. coli* (0.56 mg/mL, 86 % lignin and 14 % Cu_2O NPs). Such results highlighted the potential of L-Cu as an alternative to neutralize MDR pathogens.

1. Introduction

As a global threat to health organization systems, bacterial biofilms cause a wide range of perpetual infections of ~80 % of human infections [1]. The surface-related bacterial formation wrapped within a covered exopolysaccharide becomes resistant to chemical attacks and harsh conditions [2,3]. The bacterial matrix of biofilm formation triggers wide flexible changes in bacteria, conceding over 1000-fold resistance to conservative antibiotic medication and the host immune system [4,5]. Bacterial biofilms are essential targets for biorthogonal therapeutics and their formation is persistent in wounds and dental transplants, urinary catheters, and indwelling medical devices [6]. The biofilm matrix reinforces embedded microbial cells and deliberately delays the hydrophobic molecule's diffusion, rendering the treatment mostly difficult [7]. The treatment of these infections is also very ineffective and challenging on wounds and indwelling therapeutic devices because microbial cells are implanted in extracellular networks, making them highly resistant to harsh environmental conditions, antibiotics [8,9], and host immune response systems [10,11]. The sustained usage of antibiotics to cure those infections also increases the emergence of antibiotic-resistant strains, provoking the burden of microbial persistence in those infections [12]. Resistance has eventually been seen to nearly currently prescribed antibiotics including vancomycin, imipenem, and ceftazidime. MRSA alone kills more Americans each year than HIV/AIDS, Parkinson's disease, emphysema, and homicide combined [9]. Infection by Gram-negative pathogens including PA in healthcare settings is worrisome because they are becoming resistant to nearly all the antibiotic drug options available [9]. The modification of existing antibiotics does not completely avert the evolution of antimicrobial resistance. Hence, new classes of antimicrobial agents are urgently needed to prevent microbial adhesion and biofilm formation of emerging pathogens with antibiotic resistance [10] (see Scheme 1).

Lignin metal-based nanomaterial composites illustrate a key modality toward biofilm eradication because of their excellent antibacterial

* Corresponding author at: Bar-Ilan Institute for Nanotechnology and Advanced Materials (BINA), Bar-Ilan University, Ramat-Gan 5290002, Israel.
E-mail address: gedanken@mail.biu.ac.il (A. Gedanken).
[1] Equal contribution of authors.

https://doi.org/10.1016/j.ultsonch.2022.106241
Received 12 September 2022; Received in revised form 21 November 2022; Accepted 23 November 2022
Available online 28 November 2022

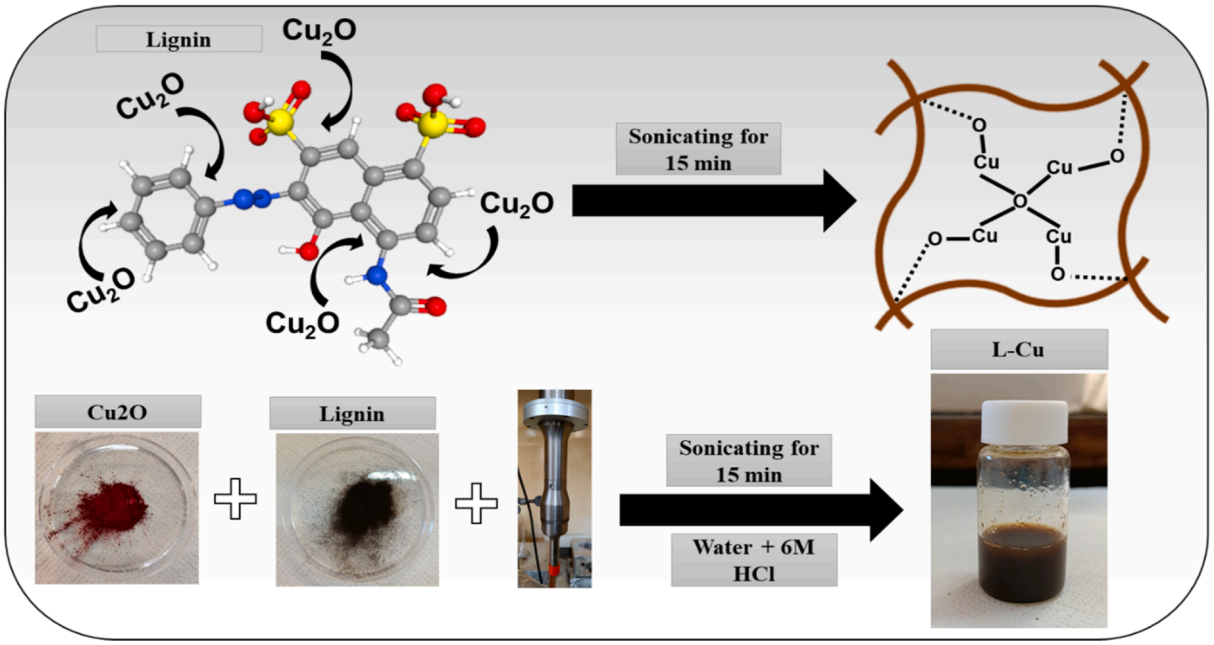

Scheme 1. Schematic illustration of lignin-capped Cu_2O synthesis.

activity, robustness, size, and tailored surface charge [13]. Bioinspired nanocomposite antibacterial materials stand out in terms of the competitive cost and scalability of their chemical counterparts [14]. The limited efficacy of antibiotics is due to their interference with the immune system along with considerable antibiotic resistance [13]. After cellulose, lignin is the second most abundant natural polymer but is hardly valuable in its macromolecular form because lignin is mainly burned for energy usage [14]. Considering its high availability and renewability, lignin represents an excellent source for the production of valuable functional molecules [13,15]. As a few examples, lignin is being utilized to improve safe design methods to provide biocompatible nanocomposite materials [16]. Lignin (L) composites have been advocated as antibacterial agents for sensitive and resistant bacteria, e.g., L-bimetallic nanoconjugate [14], aminated L-NPs (nanoparticles) [13], L-capped Ag NPs [17], Te-L-NPs [18], lignocellulose nanocrystals [19], L-hydrogels [20], L-CuS [4], Kraft L/silica–AgNPs [21] and L-PVA (polyvinyl alcohol)/chitosan [22]. Albeit lignin-based composites have been developed for antibacterial and antibacterial wound applications [17], there are very limited reports of antibiofilm treatment by L-based composites. Green procedures for fabricating L-Cu nanoparticles are appealing as they involve no chemicals, which might adversely affect plants, humans, and the environment.

This study focuses on a nanocomposite of L-Cu (lignin-Cu_2O) prepared by ultrasonication with antibiofilm applications. The L-Cu nanocomposite material is stabilized due to the formation of strong interaction between the lignin chain and the Cu_2O. Subsequently, there is a conspicuous change in the backbone of the lignin of the nanocomposites compared to the pristine Lignin. To our knowledge, this is the first effort for the formation of the L-Cu by sonochemistry. Of only relevance is the synthesis of a stable lignin nanocomposite by depositing Cu_2O into lignin by ultrasonication. This strong binding of L-Cu provides the antibiofilm properties against five selected WHO high-priority pathogens: *Escherichia coli (E. coli),* multidrug-resistant (MDR) *E. coli, Pseudomonas aeruginosa (P. aeruginosa), Staphylococcus aureus (S. aureus),* and methicillin-resistant *S. aureus* (MRSA). Based on pertinent experimental evidence, a postulated mechanism is suggested to highlight the role of the L-Cu nanocomposite, which efficiently penetrates bacterial cells and interferes with biofilm formation.

2. Characterization of materials

The L-Cu was sonicated by an ultrasonic transducer (Ultrasonic Disruptor, 20 kHz, 750 W with 30 % amplitude). The size and surface topography of the fabricated substrates and Cu_2O were characterized by environmental scanning electron microscopy (ESEM), high-resolution scanning electron microscopy (HRSEM) with an FEI Megallen 400 L microscope, and transmission electron microscopy (TEM) JEOL 2100. The phases of Cu_2O and coated substrates were probed by X-ray diffraction (XRD) (40 kV, monochromatic Cu Kα radiation: $\lambda = 0.15418$ nm). The XPS (X-ray Photoelectron Spectroscopy) peaks obtained by the Thermo Scientific Nexa spectrometer, UHV) were deconvoluted using XPSPEAK 41 software. The generation of reactive oxygen species (ROS) was examined by a Bruker ELEXSYSR500cw X-band electron paramagnetic resonance (EPR) spectrophotometer. The sonochemical process was carried out using an ultrasonic transducer (Tihorn, 20 kHz, 750 W, Sonics, and Materials VC750, USA). With a cell volume of 80 mL and an electric power of 650 W, the ultrasonic power of 29.8 W with a corresponding power density of 0.37 $W{\cdot}cm^{-3}$ was determined calorimetrically by measuring the time-dependent temperature increase in the ultrasonic vessel [23].

3. Result and discussion

The optimal conditions of the frequency, power, and efficiency have been well established in our laboratory for sonochemical coating on fabrics [23,24]. Surface & Coatings Technology 204, 54–57, 2009; J. Mater. Chem. B, 2013, 1, 1968]. First, the operating temperature was kept constant and low in this study because the gas solubility in the liquid decreases at elevated temperatures, resulting in reduced cavitation nuclei available [25]. Increasing liquid temperature also decreases the cavitation threshold, due to increased liquid vapor pressure or a decrease in surface tension or viscosity [26]. It should be noted that a temperature change can affect other parameters, and frequency for example; an increase in liquid temperature to 40 °C causes a shift of maximum H2O2 production to 613 kHz from 204 to 362 kHz [27]. A sound field consists of both standing and traveling wave components, with optimization of sonochemical yields observed in the presence of traveling waves [28]. An ultrasonic horn operating at 20 kHz consists of both traveling and standing waves [29], therefore, this setup and

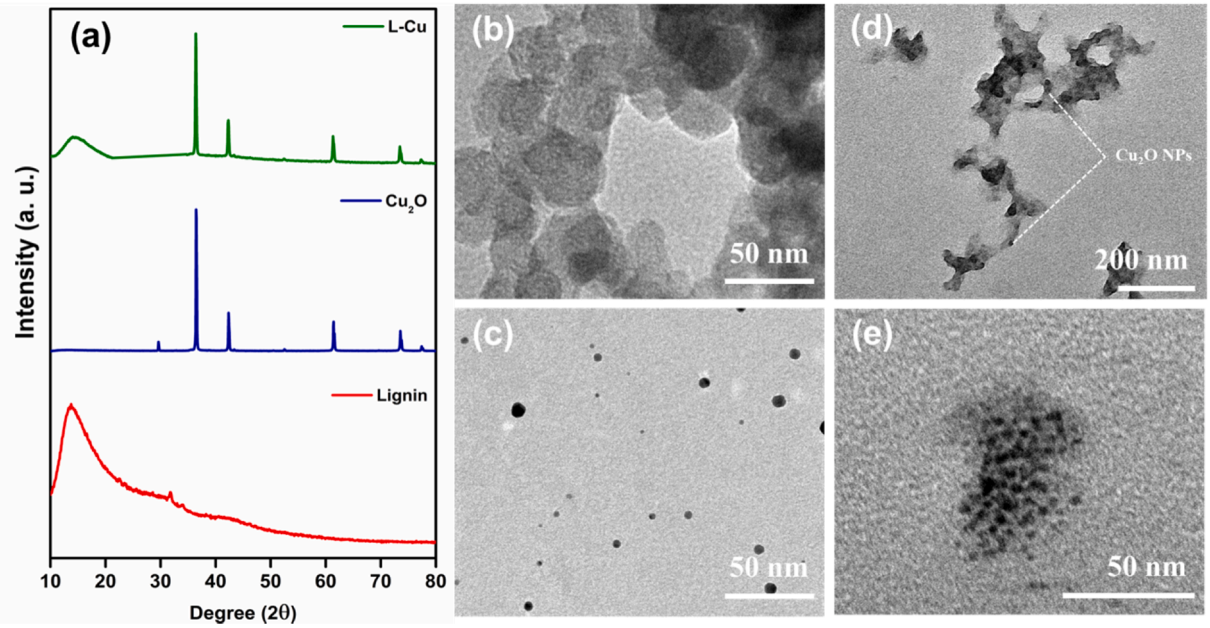

Fig. 1. (a) The XRD patterns of lignin, Cu_2O, and L-Cu, (b) TEM micrograph of lignin (c), TEM micrograph of Cu_2O NPs, (d) TEM micrograph of L-Cu, and (d) Magnified image of L-Cu.

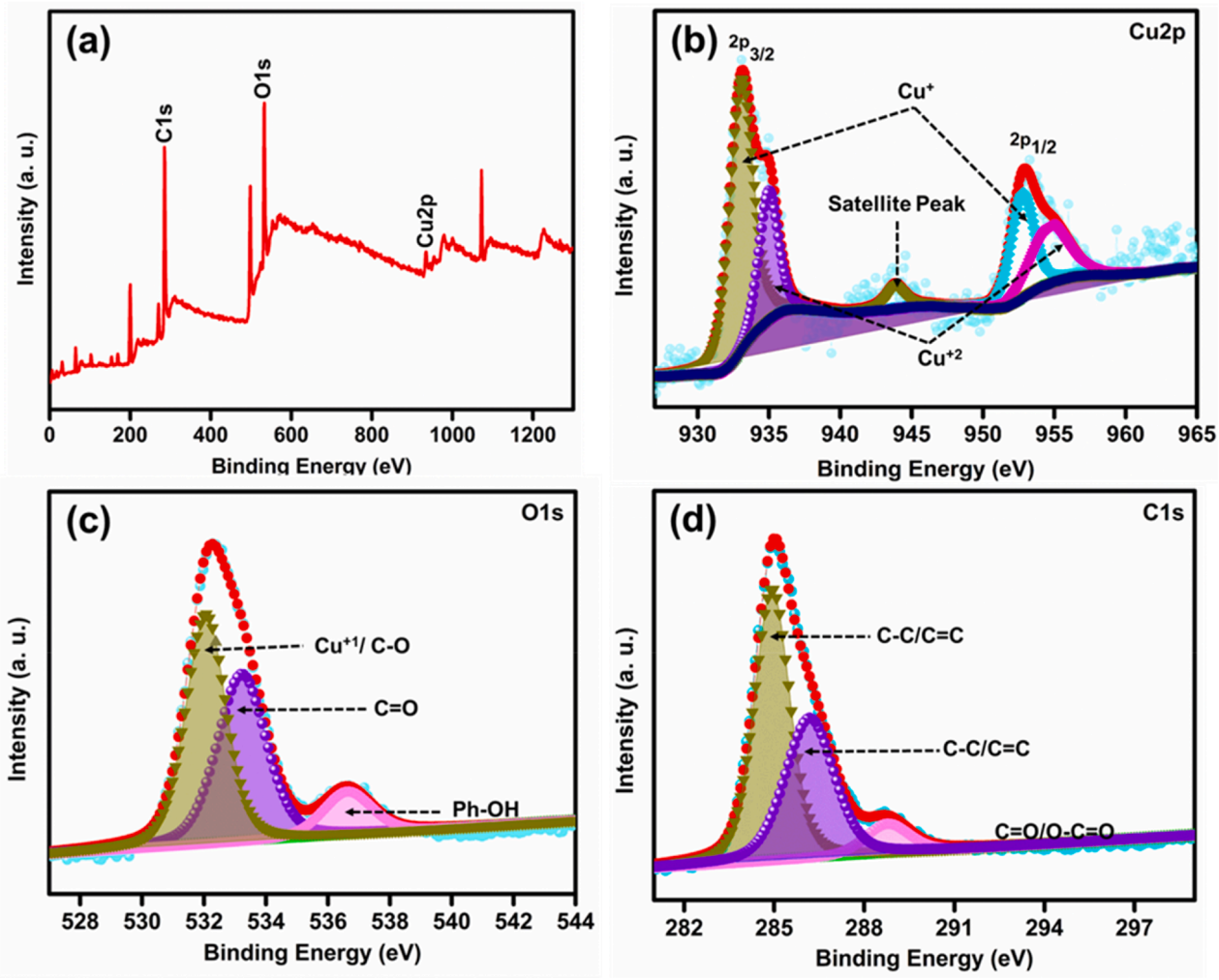

Fig. 2. (a) XPS survey spectra of L-Cu, (b-d) high-resolution spectra of Cu_2O, oxygen, and carbon.

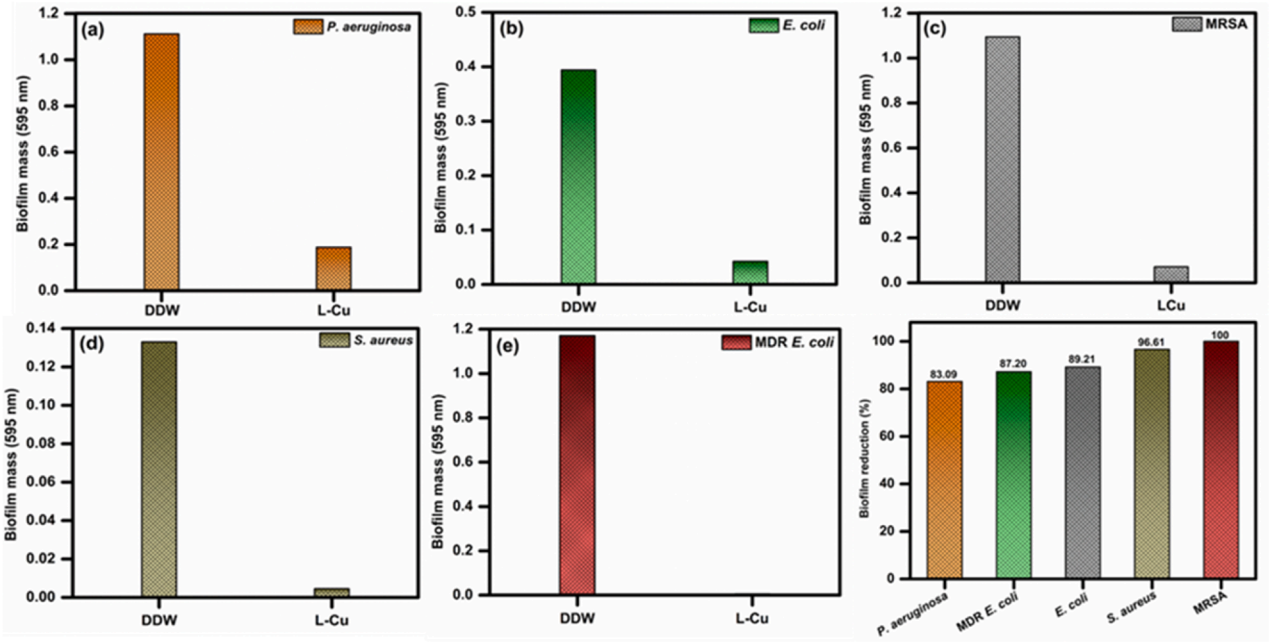

Fig. 3. Comparison of Biofilm biomass between doubly deionized water (DDW) and lignin-capped Cu_2O (L-Cu) by crystal violet staining assay (a) *Pseudomonas aeruginosa (P. aeruginosa)*, (b) multidrug-resistant *E. coli* (MDR *E. coli)*, (c) *Escherichia coli (E. coli)*, (d) *Staphylococcus aureus (S. aureus)*, and (e) methicillin-resistant *S. aureus* (MRSA), and (f) Percentage of biomass reduction by each bacterial strain.

frequency were adopted in this study with the applied electric power at 650 W, corresponding to an ultrasonic power of 29.8 W and a power density of 0.37 $W{\cdot}cm^{-3}$as mentioned earlier.

The welL-developed sonication technique [30,31] was used to synthesize lignin-Cu_2O (L-Cu). The strongly capped material is formed because of the strong ultrasonic binding interaction between lignin and Cu_2O and the product yield was 90 %. As mentioned in Table S1, Zidan et al. [32] prepared lignin nanosphere-supported cuprous oxide by stirring for 1 h. However, Gala et. al. [17] prepared lignin-capped silver nanoparticles with sonication for 2 h. Shuqi et. al. [16] reported a multistep synthesis of lignin-capped polyurethane/Ag composite. Similarly, in other reports, they used lengthy sonication or stirring approach for the preparation of lignin-based composite materials. Consequently, the binding interaction between the materials is lower by the stirring method. As compared to the reported synthesis studies, we reported a green and short-time sonochemical method for the synthesis of L-Cu, which exhibited strong biocompatibility, low cost, and excellent biofilm inhibition ability. In brief, the ultrasonic irradiation of the liquid forms the primary effects of cavitation such as bubble formation, growth, and collapse as well as heat. During the microscopic cavitation, the bubbles collapsed on the surface of the solid material, it generates powerful shock waves along with microjets which makes the effective mixing of the adjacent liquid layer. These cavitation effects are several hundred times higher in the heterogeneous than the homogeneous system. In our synthesis, ultrasonic waves stimulated the fast migration of the Cu_2O particles on the lignin surface to make a strong binding. This collision of the imprinting Cu_2O particles with the solid surface caused the local fusion with the lignin chain at the contact sites, a rationale behind the strong binding of Cu_2O particles to lignin.

In agreement with the literature, Fig. 1a shows an amorphous XRD peak of pristine lignin at 13.72° [33] and a crystallographic phase of Cu_2O NPs with six XRD peaks at 29.6°, 36.4°, 42.4°, 61.3°, 73.5°, and 77.4° (JCPDS No. 05–0667) [34]. The L-Cu nanocomposite displayed a noticeable peak at 14.27° for lignin and 36.4°, 42.4°, 61.3°, 73.5°, and 77.4° diffraction peaks corresponding to Cu_2O NPs, these diffraction peaks indicated that due to strong capping treatment of Cu_2O NPs with lignin, a new phase was formed, appreciably even though a very small amount of the Cu_2O powder was used for the synthesis of L-Cu. Cu_2O NPs and alkaline lignin are positively charged at neutral pH [35]. Thus, hydrophobic interactions between lignin and Cu_2O played an important role in the formation of stable L-Cu. A broad peak observed for lignin was anticipated as lignin is a highly branched biopolymer composed of phenol units with strong intramolecular bonding. Ultrasound energy has been used to remove and purify lignin from different sources of biomass and this procedure presents no significant modifications of lignin in terms of composition, structure, [36] or molecular weight [37]. Lignin nanoparticles can be synthesized by ultrasonication; however, the process is lengthy, 60 min at 20 kHz frequency and 600 W [38], compared to a total time of 15 min used in this study using a mixture of lignin and Cu_2O powder.

TEM imaging illustrated the polyhedral morphology of lignin and a spherical shape for Cu_2O (10–20 nm in diameter) NPs (Fig. 1b,c), which were capped on lignin (Fig. 1 d, e). L-Cu exhibited three XPS peaks at 281.1 (C1s), 532.39 (O1s), and 933.27(Cu2p) eV (Fig. 2a). High-resolution spectra of Cu2p stemming from Cu_2O NPs encompassed the corresponding peaks of Cu^+ ($2p_{3/2}$, $2p_{1/2}$), Cu^{+2} ($2p_{3/2}$, $2p_{1/2}$), and five satellite peaks at 933.06 (Cu^+), 934.98, 943.87 (Cu^{+2}), 952.76 (Cu^+), and 954.67 eV (Cu^{+2}) (Fig. 2b). The unassigned peak at 943.87 eV was associated with a satellite peak [39]. Fig. 2c shows the attributed peaks of O1s at 532.06, 533.22, and 536.63 eV, which were assigned to Cu^+/C—O, C═O, and Ph═O [39,40]. The C1s high-resolution peaks at 284.93 eV, 286.18 eV, and 288.77 eV were assigned to the C—C/C═C, C-OH, and C═O/O-C═O bond of lignin (Fig. 2d) [41]. The structural units in lignin are *p*-hydroxyphenyl, guaiacyl, and syringyl [42] as lignin is a highly branched polymer of three precursors: *p*-coumaryl alcohol, coiferyl alcohol, and sinapyl alcohol [43]. Such precursors are linked by β-O-4 aryl ethers, β-β (resinols), β-5 (phenylcoumarans), β-1 (spirodienones), and 5–5 and 4-O-5 linkages.

4. Biofilm inhibition by L-Cu

Lignin has some antimicrobial activities owing to the presence of the methoxy and phenolic hydroxyl groups. However, lignins prepared from different biomass sources and preparation methods have different 3D structures and different antimicrobial activities [44]. In this work, alkali lignin was used without any treatment or purification as purified lignin

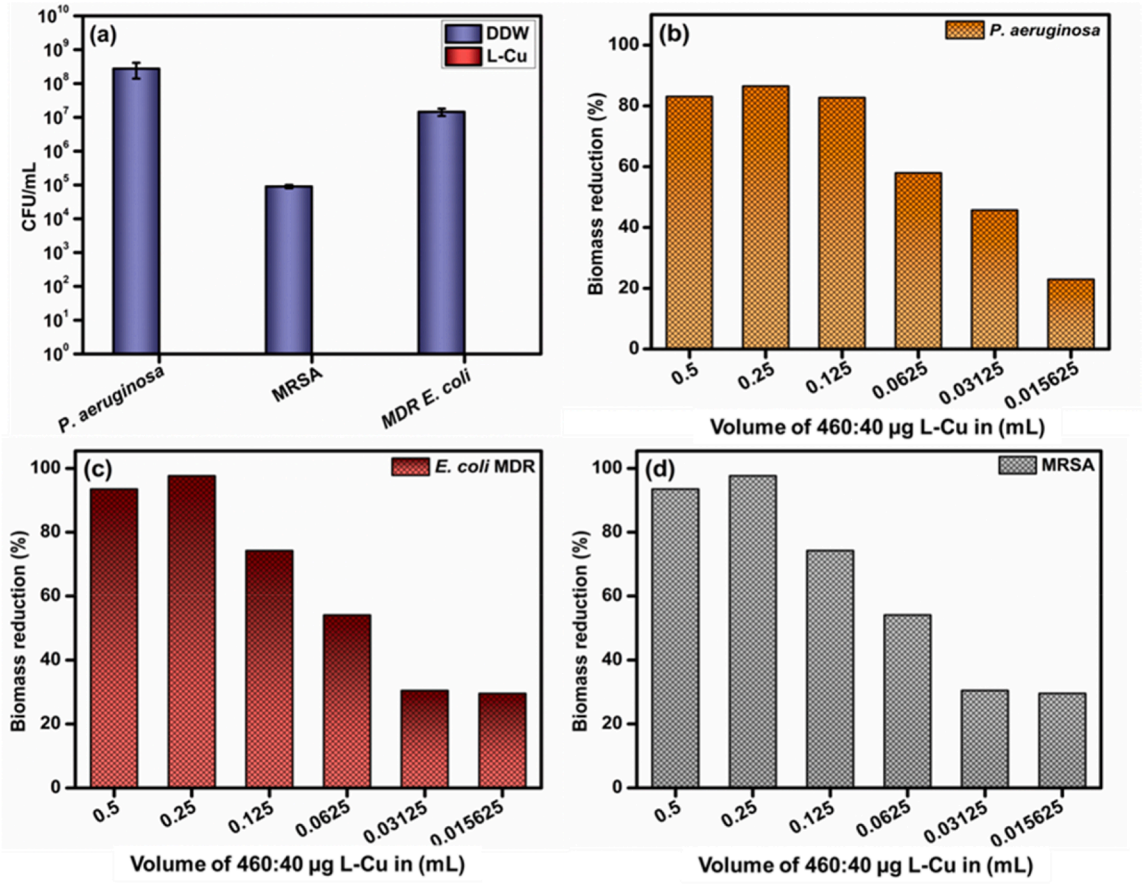

Fig. 4. (a) CFU of Planktonic viable cells after 18 h incubation with L-Cu against *P. aeruginosa*, MDR *E. coli*, and *MRSA*, (b–d) concentration-dependent planktonic cell reduction percentage of *P. aeruginosa*, MDR *E. coli*, and *MRSA*.

has a reduced effect on antimicrobial activity [45]. Unmodified lignin is also more effective against gram-positive *Bacillus* species than against gram-negative *Klebsiella* species [46]. There is some conflicting information as lignins obtained from different sources and preparation methods do not inhibit the growth of *E. coli* [47]. Therefore, this work focused on a nanocomposite of unmodified lignin and Cu_2O NPs with potential antimicrobial and antibiofilm properties. There are two types of industrial lignin, Kraft lignin and ammonium lignosulfonates [48]. Kraft lignin is selected in this study because it accounts for about 85 % of the total lignin production in the world. Kraft lignin is used as received as purified Kraft lignin obtained via solvent extraction exhibited a negative effect on the antimicrobial activity as mentioned earlier.

The antibiofilm property of L-Cu was examined against five common pathogens and the crystal violet (CV) assay was used to measure the biofilm eradication activity of L-Cu. The absorbance of a biofilm after being treated with L-Cu was measured (Fig. 3a-e) and the percentage biofilm reduction was calculated. Fig. 3(f) reveals the superior biofilm mass reduction potential of L-Cu varied from 83 to 100 % against *E. coli*, MDR *E. coli*, *P. aeruginosa*, *S. aureus*, and MRSA and after 18 h incubation with the preformed biofilms. Among them, the percentage of biofilm biomass reduction was predominant (95–100 %) for *S. aureus* and MRSA. In all cases, over 80 % inhibition was observed in the presence of L-Cu at 460:40 µg in 500 µL (L-Cu, 1 mg/mL). These results evinced that L-Cu exhibited excellent antibiofilm activities against all the tested pathogens. Overall, L-Cu displays the following order of antibiofilm activity against MRSA > *S. aureus* > *E. coli* > MDR *E. coli* > *P. aeruginosa*. Differences in the level of antimicrobial activity were somewhat anticipated as this property is governed by the bacterial gram characteristics, zeta potential, the ability to build exopolysaccharides, and membrane permeability. Any difference in such factors would cause variation in the antimicrobial activity against different bacteria.

The inhibitory effect of L-Cu on planktonic viable cells was observed by spread on an agar plate after 18 h incubation with L-Cu and a corresponding photograph was captured (Fig. S1). With the comparison of control (DDW), L-Cu inhibited completely the growth of *P. aeruginosa*, *MRSA*, and MDR *E. coli* at L-Cu at 460:40 µg in 500 µL (L-Cu). In the case of DDW-treated planktonic cells for MRSA, about 2.5 less log reduction was observed when compared with *P. aeruginosa* and MDR *E. coli* (Fig. 4a). A corresponding percentage of bacterial inhibition of planktonic cells was also performed in Fig. S2(a). L-Cu at 460:40 µg in 500 µL has superior activity in clearance for all three planktonic cells' survival. The MIC is defined as the minimal concentration at which there is no obvious bacterial growth. For the determination of MICs, the experiment was performed for concentration-dependent planktonic cell inhibition activity L-Cu and DDW (as a control) treated. A corresponding percentage of bacterial reduction observed by using AB_{595} is shown in Fig. S2 (b). The percentage of planktonic viable cell reduction for selected pathogens and results are described in Fig. 4(b-d). The planktonic cell mass of drug-resistant pathogens MRSA and MDR *E. coli* were decreased by about 98 % and 99 % upon contact with L-Cu nanoparticles with a concentration of 230:20 µg and 460:40 µg (L-Cu). The MIC value for MDR *E. coli* planktonic clearance is recorded higher than (double times) the MIC value for MRSA and sensitive *P. aeruginosa,* indicating the superior planktonic bacterial clearance for MRSA and *P. aeruginosa* at minimal concentrations. In the case of *P. aeruginosa*, the biofilm mass reduction was attained at only ~83 % when incubated with a concentration of 230:20 µg. The largest planktonic viable cell reduction difference was observed against MRSA, demonstrating that L-Cu exhibited both the highest biofilm eradication activity as well as planktonic bacterial killing against MRSA (Fig. 3f and 4d). The overall MIC (minimum

Table 1
MIC values for biofilm eradication and planktonic removal.

Bacteria's	L-Cu concentration for biofilm inhibition (1 mg/mL)	MIC of L-Cu for planktonic killing (mg/mL)
P. aeruginosa	(0.920 L + 0.080 Cu)	0.3 (0.260 L + 0.04 Cu)
MDR E. coli	(0.920 L + 0.080 Cu)	0.56 (0.48 L + 0.08 Cu)
S. aureus	(0.920 L + 0.080 Cu)	0.56 (0.48 L + 0.08 Cu)
MRSA	(0.920 L + 0.080 Cu)	0.3 (0.260 L + 0.040 Cu)

inhibition concentration) for biofilm eradication and planktonic killing by L-Cu is presented in Table 1. The MIC values were comparable to those of cationic lignin-based hyperbranched polymers; 128 ppm or 0.128 mg/mL [49]. The L-Cu composite displayed a broad-spectrum antimicrobial activity against Gram-negative MDR *E. coli* and MRSA strains without any significant shift in the MIC values. This is an important finding as the nanocomposite could be further investigated as a new class of antibiotics for treating bacterial infections. It is logical to anticipate low MICs by fusing NPs with the aforementioned cationic lignin-based hyperbranched polymers.

5. A postulated mechanism

Lignin composed of aromatic rings with hydroxy and methoxy functional groups has been known as a binding substance for enzymes, particularly cellulases by hydrophobic [50] and electrostatic [51] interactions. The binding event is also reinforced by the hydrogen bonding of the cellular biomolecules with several functional groups of lignin. In the plant cell wall, lignin is associated with carbohydrate polymers. The bacterial membrane comprises a lipid bilayer and associated proteins and the major lipid species are phospholipids and glucolipids. A postulated mechanism of antimicrobial activities of L-Cu is illustrated in Fig. 5.

Based on the positive charge of lignin at neutral pH as discussed earlier, lignin exhibits electrostatic interactions with negatively charged bacteria. The hydrophobic nature of lignin plays an important role in its binding to the phospholipid domain in the bacterial membrane. The polyphenolic structure of lignin together with O-containing functional groups (methoxyl and epoxy groups) is potentially responsible for these activities [52]. Lignin with high phenolic hydroxyl contents can damage bacterial cell walls [53], resulting in the leakage of the bacterial cytosol. The degree of damage is proportional to increasing concentration and lignin has s a significant influence on deconstructing the cell wall of several bacteria such as *Bacillus subtilis*, *E. coli*, *Salmonella*, *Listeria*, *S. aureus*, and *Klebsiella* [54]. Another antimicrobial effect of lignin is the creation of a low pH environment on the cell membrane to destroy the proton dynamics of the cell membrane [54]. Similarly, Cu_2O NPs with a positive charge are also bound to bacteria with an opposite charge. The binding event interferes with cell wall synthesis and membrane function. Copper oxide nanoparticles with potential application as antimicrobial agents have been demonstrated by several groups [55–57]. Among some plausible antimicrobial mechanisms, the generation of enhanced ROS (reactive oxygen species) plays an important role in bacterial eradication (Fig S3). Therefore, this study focused on the synthesis of a nanocomposite of lignin-Cu_2O NPs with anticipated enhanced antimicrobial and antibiofilm properties. Unmodified lignin (MW = 5,070) and three fractionated lignins (MW = 7,260, 3,480, and 1,810) can inhibit the growth of Gram-negative bacteria, and Gram-positive bacteria by destroying the bacterial cell wall. The fractionation by anhydrous acetone results in higher MW lignin (7,260), whereas two lower MW lignin fragments are attained by subsequent fractionation with 50 % acetone and 37.5 % hexanes [54]. However, the lignin fraction with the lowest molecular weight and highest phenolic hydroxyl content shows the best performance [58]. This study confirmed that unmodified lignin (MW = 10 kDa) formed a nanocomposite with Cu_2O NPs displayed strong antimicrobial and antibiofilm activities against both 5 g-positive and negative bacteria. MDR *E. coli* has become a major public health concern in many countries and PA causes devastating acute and chronic infections in subjects with compromised immune systems. Nevertheless, lignin-Cu composites prepared from lignin with various molecular weights might affect the film formation and their corresponding antimicrobial activities, a subject of future endeavors.

The experiment was then conducted to probe the morphological change in bacterial cells by ESEM. The bacterial cell death before and after treatment with L-Cu is displayed in Fig. 6a-f. The micrographs unraveled clear morphological shapes for all tested pathogens without

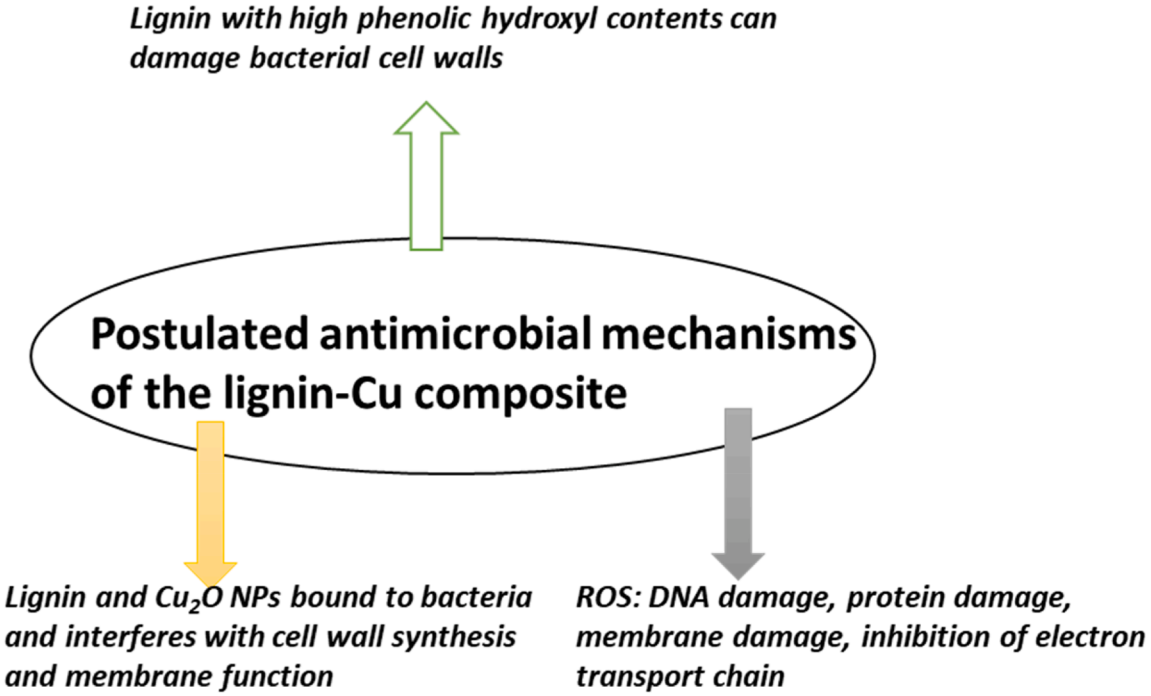

Fig. 5. A postulated mechanism for antimicrobial properties of the lignin-Cu composite.

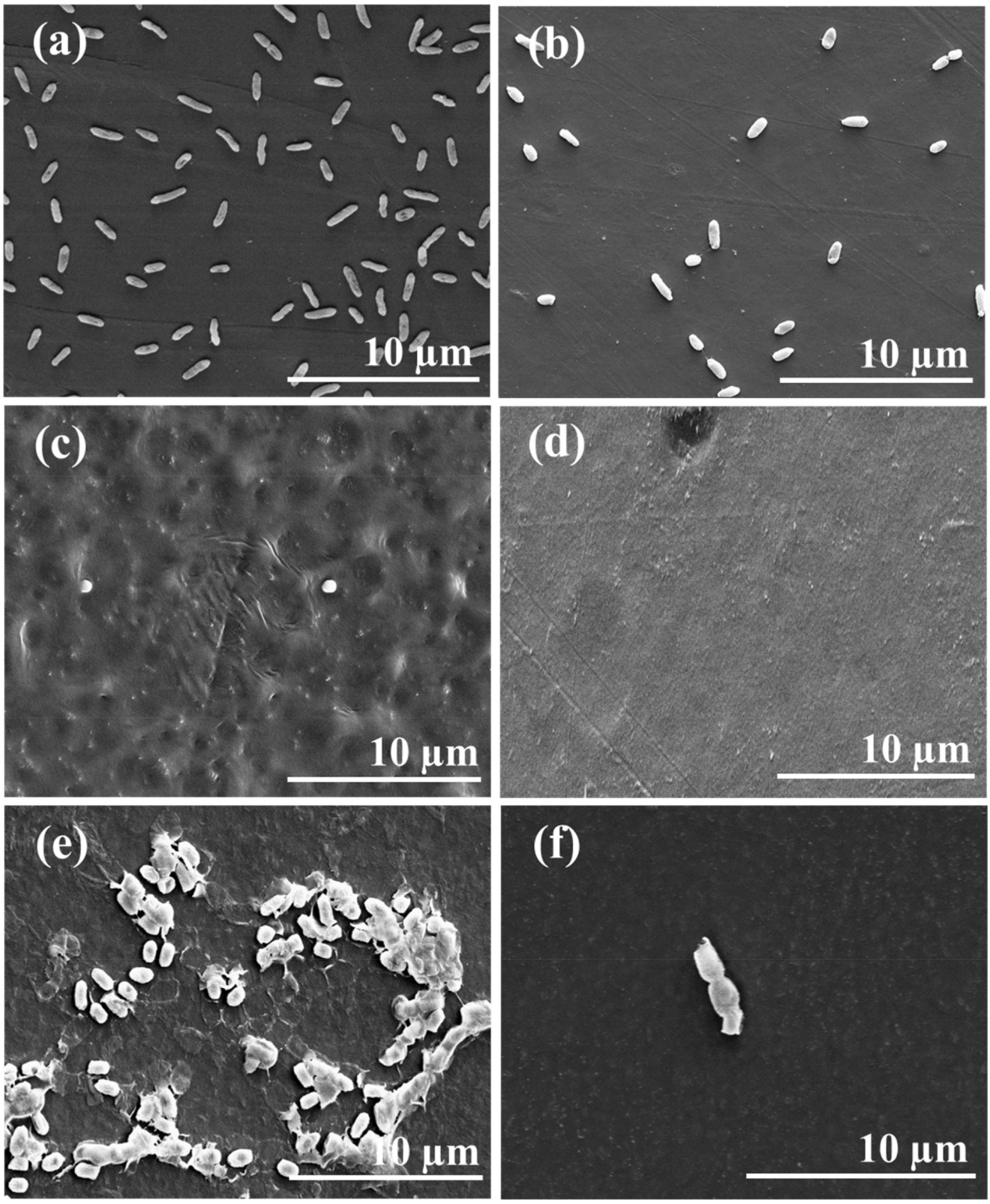

Fig. 6. ESEM micrographs of DDW and L-Cu treated viable cells, (a) DDW treated *P. aeruginosa* cells, (b) L-Cu treated *P. aeruginosa cells*, (c) DDW treated MRSA cells, (d) L-Cu treated MRSA cells, (e) DDW treated MDR *E. coli* cells, and (f) L-Cu treated MDR *E. coli* cells.

any noticeable membrane damage. In contrast, the cell damage of PA, MRSA, and MDR *E. coli* is shown in Fig. 6b, d, and f. After the treatment with L-Cu, the bacterial cells lost the integrated structural morphology, while no bacterial cell was viewed after treatment with the material. The kraft lignin was used in this study over another common lignin, known as organosolv lignin because the former exhibits higher antimicrobial activities due to its lower carbohydrate content and the presence of sulfur-containing derivatives [59]. The organosolv lignin is highly pure and sulfuric-free with minimal modification as lignin is simply dissolved in an organic solvent, e.g., acetic acid, ketone, and ester [60]. Of further interest is the synthesis of lignin composites with other polymers, e.g., poly(butylene succinate) [61], alginate [62], and poly(vinyl alcohol) (PVA) [63] to promote antimicrobial activities. Lignin, lignin derivatives, and their nanocomposites will emerge as a new class of

antimicrobial or anti-biofouling materials. The disruption of PA, MRSA, and MDR *E. coli* by L-Cu is an important finding as with an outer cell membrane, they are harder to eradicate than Gram-positive counterparts. However, an exact mechanism regarding the antimicrobial and antifilm activities of lignin and its composites remains a focus of ongoing studies.

6. Conclusion

Altogether, the lignin-capped Cu_2O prepared by facile sonochemistry displayed antibiofilm properties against five common pathogens. resistant biofilm. L-Cu exhibited over 90 % biofilm *S. aureus*, MRSA, *E. coli*, MDR *E. coli*, and *P. aeruginosa* and reached a complete biofilm mass reduction in 24 h. The excellent performance of L-Cu can be due to the combination and binding ability of nanocatalysts against sensitive and drug-resistant pathogens. Overall, the simple, eco-friendly, inexpensive L-Cu has great potential to provide an effective platform for antibacterial, antibiofilm applications, which may be further used for clinical translation. The antimicrobial and antiradical activities of lignin are also of great interest for food packaging, food additives, medical textile, and other medical fields. It is important to develop new agents able to prevent microbial adhesion and proliferation on material surfaces with subsequent negative effects. The antimicrobial/antibiofilm potential of naturally derived underutilized lignin remains a subject of future endeavors. Strong antimicrobial properties allied with their excellent biocompatibility and low cytotoxicity, make lignin and its nanocomposites with metallic nanoparticles and/or polymers good for diverse applications. However, both unmodified and modified lignin still present lower antibacterial activity than standard antibiotics. Thus, the advancement of lignin, lignin derivatives, and their composites as effective antimicrobial agents with minimal cytotoxicity remains a subject of future undertakings.

CRediT authorship contribution statement

Moorthy Maruthapandi: Methodology, Writing – original draft. **Akanksha Gupta:** Methodology, Writing – original draft. **Arumugam Saravanan:** Data curation. **Gila Jacobi:** . **Ehud Banin:** . **John H.T. Luong:** . **Aharon Gedanken:** .

Declaration of Competing Interest

The authors declare that they have no known competing financial interests or personal relationships that could have appeared to influence the work reported in this paper.

Acknowledgments

The authors would like to acknowledge Prof. Shulamit Michaeli and Saurav Aryal for cytotoxicity support.

Appendix A. Supplementary data

Supplementary data to this article can be found online at https://doi.org/10.1016/j.ultsonch.2022.106241.

References

[1] T.-F. Mah, G.A. O'Toole, Mechanisms of biofilm resistance to antimicrobial agents, Trends Microbiol. 9 (1) (2001) 34–39.
[2] J.D. Bryers, Medical biofilms, Biotechnol. Bioeng. 100 (1) (2008) 1–18.
[3] D.J. Musk, P.J. Hergenrother, Chemical countermeasures for the control of bacterial biofilms: effective compounds and promising targets, Curr. Med. Chem. 13 (2006) 2163–2177.
[4] Y. Xie, Y. Qian, Z. Li, Z. Liang, W. Liu, D. Yang, X. Qiu, Near-infrared-activated efficient bacteria-killing by lignin-based copper sulfide nanocomposites with an enhanced photothermal effect and peroxidase-like activity, ACS Sustain. Chem. Eng. 9 (18) (2021) 6479–6488.
[5] M. Ramasamy, J. Lee, Recent nanotechnology approaches for prevention and treatment of biofilm-associated infections on medical devices, BioMed Res. Int. 1851242 (2016) 1–17.
[6] R. Donlan, Biofilms and device-associated infections, Emerging, Infect. Dis. 7 (2) (2001) 277–281.
[7] H.C. Flemming, T.R. Neu, D.J. Wozniak, The EPS matrix: the "house of biofilm cells, J. Bacteriol. 189 (2007) 7945–7947.
[8] G.M. Viola, R.O. Darouiche, Cardiovascular implantable device infections, Curr. Infect. Dis. Rep. 13 (4) (2011) 333–342.
[9] C.L. Ventola, The antibiotic resistance crisis: part 1: causes and threats, PT 40 (2015) 277–283.
[10] A. Vishwakarma, F. Dang, A. Ferrell, H. Barton, A. Joy, Peptidomimetic polyurethanes inhibit bacterial biofilm formation and disrupt surface established biofilms, JACS 143 (2021) 9440–9449.
[11] R.D. Wolcott, D.D. Rhoads, M.E. Bennett, B.M. Wolcott, L. Gogokhia, J. W. Costerton, S.E. Dowd, Chronic wounds and the medical biofilm paradigm, J. Wound Care. 19 (2) (2010) 45–53.
[12] L.-S. Wang, A. Gupta, V.M. Rotello, Nanomaterials for the treatment of bacterial biofilms, ACS Infect. Dis. 2 (1) (2016) 3–4.
[13] W. Yang, H. Ding, G. Qi, J. Guo, F. Xu, C. Li, D. Puglia, J. Kenny, P. Ma, Enhancing the radical scavenging activity and UV resistance of lignin nanoparticles via surface mannich amination toward a biobased antioxidant, Biomacromolecules. 22 (6) (2021) 2693–2701.
[14] Y. Zhang, M. Naebe, Lignin: A review on structure, properties, and applications as a light-colored UV absorber, ACS Sustain. Chem. Eng. 9 (2021) 1427–1442.
[15] S. Chandna, N.S. Thakur, R. Kaur, J. Bhaumik, Lignin–bimetallic nanoconjugate doped pH-responsive hydrogels for laser-assisted antimicrobial photodynamic therapy, Biomacromolecules. 21 (8) (2020) 3216–3230.
[16] S. Li, Y. Zhang, X. Ma, S. Qiu, J. Chen, G. Lu, Z. Jia, J. Zhu, Q. Yang, J. Chen, Y. Wei, Antimicrobial lignin-based polyurethane/ag composite foams for improving wound healing, Biomacromolecules. 23 (4) (2022) 1622–1632.
[17] A.G. Morena, I. Stefanov, K. Ivanova, S. Pérez-Rafael, M. Sánchez-Soto, T. Tzanov, Antibacterial polyurethane foams with incorporated lignin-capped silver nanoparticles for chronic wound treatment, Ind. Eng. Chem. Res. 59 (10) (2020) 4504–4514.
[18] A.G. Morena, A. Bassegoda, J. Hoyo, T. Tzanov, Hybrid tellurium–lignin nanoparticles with enhanced antibacterial properties, ACS Appl. Mater. Interfaces. 13 (13) (2021) 14885–14893.
[19] D. Georgouvelas, B. Jalvo, L. Valencia, W. Papawassiliou, A.J. Pell, U. Edlund, A. P. Mathew, Residual lignin and zwitterionic polymer grafts on cellulose nanocrystals for antifouling and antibacterial applications, ACS Appl. Polym. Mater. 2 (8) (2020) 3060–3071.
[20] S. Afewerki, X. Wang, G.U. Ruiz-Esparza, C.-W. Tai, X. Kong, S. Zhou, K. Welch, P. Huang, R. Bengtsson, C. Xu, M. Strømme, Combined catalysis for engineering bioinspired, lignin-based, long-lasting, adhesive, self-mending, antimicrobial hydrogels, ACS Nano. 14 (12) (2020) 17004–17017.
[21] Ł. Klapiszewski, T. Rzemieniecki, M. Krawczyk, D. Malina, M. Norman, J. Zdarta, I. Majchrzak, A. Dobrowolska, K. Czaczyk, T. Jesionowski, Kraft lignin/silica–AgNPs as a functional material with antibacterial activity, Colloids Surf. B. 134 (2015) 220–228.
[22] W. Yang, J.S. Owczarek, E. Fortunati, M. Kozanecki, A. Mazzaglia, G.M. Balestra, J. M. Kenny, L. Torre, D. Puglia, Antioxidant and antibacterial lignin nanoparticles in polyvinyl alcohol/chitosan films for active packaging, Ind Crops Prod. 94 (2016) 800–811.
[23] P. Petkova, A. Francesko, M.M. Fernandes, E. Mendoza, I. Perelshtein, A. Gedanken, T. Tzanov, Sonochemical coating of textiles with hybrid ZnO/chitosan antimicrobial nanoparticles, ACS Appl. Mater. Interf. 6 (2014) 1164–1172.
[24] I. Perelshteina, G. Applerota, N. Perkasa, E. Wehrschuetz-Siglb, A. Hasmannb, G. Guebitzb, A. Gedanken, CuO–cotton nanocomposite: Formation, morphology, and antibacterial activity, Surf. Coat. Technol. 204 (2009) 54–57.
[25] E.A. Hemmingsen, Cavitation in gas - supersaturated solutions, J. Appl. Phys. 46 (1) (1975) 213–218.
[26] T.J. Mason, J.P. Lorimer, Applied Sonochemistry, Wiley-VCH Verlag GmbH & Co, KGaA, 2002.
[27] R. Pflieger, T. Chave, G. Vite, L. Jouve, S.I. Nikitenko, Effect of operational conditions on sonoluminescence and kinetics of H_2O_2 formation during the sonolysis of water in the presence of Ar/O2 gas mixture, Ultrason. Sonochem. 26 (2015) 169–175.
[28] M.J. Bussemaker, D. Zhang, A phenomenological investigation into the opposing effects of fluid flow on sonochemical activity at different frequency and power settings. 1. Overhead stirring, Ultrason. Sonochem. 21 (1) (2014) 436–445.
[29] A. Henglein, Chemical effects of continuous and pulsed ultrasound in aqueous solutions, Ultrason. Sonochem. 2 (2) (1995) S115–S121.
[30] M. Maruthapandi, L. Eswaran, J.H.T. Luong, A. Gedanken, Sonochemical preparation of polyaniline@ TiO_2 and polyaniline@ SiO_2 for the removal of anionic and cationic dyes, Ultrason. Sonochem. 62 (2020), 104864.
[31] M. Maruthapandi, A. Saravanan, S. Manoj, J.H.T. Luong, A. Gedanken, Facile ultrasonic preparation of a polypyrrole membrane as an absorbent for efficient oil-water separation and as an antimicrobial agent, Ultrason. Sonochem. 78 (2021), 105746.
[32] Z. Zhou, X. Peng, L. Zhong, X. Li, R. Sun, Lignin nanosphere-supported cuprous oxide as an efficient catalyst for Huisgen [3+2] cycloadditions under relatively mild conditions, Polymers 10 (2018) 724.
[33] S. Afewerki, X. Wang, G.U. Ruiz-Esparza, C.W. Tai, X. Kong, S. Zhou, K. Welch, P. Huang, R. Bengtsson, C. Xu, M. Strømme, Combined catalysis for engineering

bioinspired, lignin-based, long-lasting, adhesive, self-mending, antimicrobial hydrogels, ACS Nano. 14 (2020) 17004–17017.
[34] Q. He, Y. Tian, Y. Wu, J. Liu, G. Li, P. Deng, D. Chen, Electrochemical sensor for rapid and sensitive detection of tryptophan by a Cu_2O nanoparticles-coated reduced graphene oxide nanocomposite, Biomolecules. 9 (2019) 176.
[35] Z. Wang, N. Bo, Y. Liu, G. Yang, Y. Liu, Y. Zhao, Preparation of lignin-based anion exchangers and their utilization for nitrate removal, BioResources 8 (2013) 3505–3517.
[36] A. Garcia, X. Erdocia, M.G. Alriols, J. Labidi, Effect of ultrasound treatment on the physicochemical properties of alkaline lignin, Chem. Eng. Process. 62 (2012) 150–158.
[37] T. Wells, M. Kosa, A.J. Ragauskas, Polymerization of Kraft lignin via ultrasonication for high-molecular-weight applications, Ultrason Sonochem. 20 (6) (2013) 1463–1469.
[38] I.A. Gilca, V.I. Popa, C. Crestini, Obtaining lignin nanoparticles by sonication, Ultrason Sonochem. 23 (2015) 369–375.
[39] X. Ma, J. Zhang, B. Wang, Q. Li, S. Chu, Hierarchical Cu_2O foam/g-C_3N_4 photocathode for photoelectrochemical hydrogen production, Appl. Surf. Sci. 427 (2018) 907–916.
[40] A.A. Myint, H.W. Lee, B. Seo, W.-S. Son, J. Yoon, T.J. Yoon, H.J. Park, J. Yu, J. Yoon, Y.-W. Lee, One pot synthesis of environmentally friendly lignin nanoparticles with compressed liquid carbon dioxide as an antisolvent, Green Chem. 18 (7) (2016) 2129–2146.
[41] M. Arefmanesh, T.V. Vuong, J.K. Mobley, M. Alinejad, E.R. Master, M. Nejad, Bromide-based ionic liquid treatment of hardwood organosolv lignin yielded a more reactive biobased polyol, Ind. Eng. Chem. Res. 59 (42) (2020) 18740–18747.
[42] T.D. Bugg, M. Ahmad, E.M. Hardiman, R. Rahmanpour, Pathways for degradation of lignin in bacteria and fungi, Nat. Prod. Rep. 28 (2011) 1883–1896.
[43] S. Laurichesse, L. Avérous, Chemical modification of lignins: towards biobased polymers, Prog. Polym. Sci. 39 (7) (2014) 1266–1290.
[44] W. Yang, E. Fortunati, F. Dominici, J.M. Kenny, G. Giovanale, A. Mazzaglia, G. M. Balestra, D. Puglia, Effect of cellulose and lignin on disintegration, antimicrobial and antioxidant properties of PLA active films, Int. J. Biol. Macromol. 89 (2016) 360–368.
[45] A. Alzagameem, S.E. Klein, M. Bergs, X.T. Do, I. Korte, S. Dohlen, C. Hüwe, J. Kreyenschmidt, B. Kamm, M. Larkins, M. Schulze, Antimicrobial activity of lignin and lignin-derived cellulose and chitosan composites against selected pathogenic and spoilage microorganisms, Polymers 11 (2019) 670.
[46] R. Kaur, S.K. Uppal, P. Sharma, Antioxidant and antibacterial activities of sugarcane bagasse lignin and chemically modified lignins, Sugar Tech. 19 (6) (2017) 675–680.
[47] Abla Al-Zagameem, Antioxidant and antimicrobial properties of lignin and lignin-based composites for active food packaging applications. Dr. rer. nat. (PhD) Thesis, Von der Fakultät für Umwelt und Naturwissenschaften der Brandenburgischen Technischen Universität Cottbus-Senftenberg zur Erlangung des akademischen Grades eines. 2020.
[48] A. Duval, S. Molina-Boisseau, C. Chirat, Comparison of Kraft lignin and lignosulfonates addition to wheat gluten-based materials: mechanical and thermal properties, Ind. Crops Products 49 (2013) 66–74.
[49] P.L. Chee, C. Owh, M. Venkatesh, M.H. Periayah, Z. Zhang, P.Y. Michelle Yew, H. Ruan, R. Lakshminarayanan, D. Kai, X.J. Loh, Cationic lignin-based hyperbranched polymers to circumvent drug resistance in *Pseudomonas keratitis*, ACS Biomater. Sci. Eng. 7 (9) (2021) 4659–4668.
[50] D.W. Sammond, J.M. Yarbrough, E. Mansfield, Y.J. Bomble, S.E. Hobdey, S. R. Decker, L.E. Taylor, M.G. Resch, J.J. Bozell, M.E. Himmel, T.B. Vinzant, M. F. Crowley, Predicting enzyme adsorption to lignin films by calculating enzyme surface hydrophobicity, J. Biol. Chem. 289 (30) (2014) 20960–20969.
[51] M.M. Bradford, A rapid and sensitive method for the quantitation of microgram quantities of protein utilizing the principle of protein-dye binding, Anal. Biochem. 72 (1-2) (1976) 248–254.
[52] J.S. Lupoi, S. Singh, R. Parthasarathi, B.A. Simmons, R.J. Henry, Recent innovations in analytical methods for the qualitative and quantitative assessment of lignin, Renew. Sustain. Energy Rev. 49 (2015) 871–906.
[53] B. Jiang, H. Chen, H. Zhao, W. Wu, Y. Jin, Structural features and antioxidant behavior of lignins successively extracted from ginkgo shells (*Ginkgo biloba* L), Int. J. Biol. Macromol. 163 (2020) 694–701.
[54] J. Yun, L. Wei, W. Li, D. Gong, H. Qin, X. Feng, G. Li, Z. Ling, P. Wang, B. Yin, Isolating high antimicrobial ability lignin from bamboo kraft lignin by organosolv fractionation, Front. Bioeng. Biotechnol. 9 (2021), 683796.
[55] F.A. Bezza, S.M. Tichapondwa, E.M.N. Chirwa, Fabrication of monodispersed copper oxide nanoparticles with potential application as antimicrobial agents, Sci. Rep. 10 (2020) 16680.
[56] Y.H. Hsueh, P.H. Tsai, K.S. Lin, pH-dependent antimicrobial properties of copper oxide nanoparticles in *Staphylococcus aureus*, Int. J. Mol. Sci. 18 (2017) 793.
[57] M. Maruthapandi, A. Saravanan, P. Das, M. Natan, G. Jacobi, E. Banin, J.H. T. Luong, A. Gedanken, Antimicrobial activities of Zn-doped CuO microparticles decorated on polydopamine against sensitive and antibiotic-resistant bacteria, ACS Appl. Pol. Mater. 2 (12) (2020) 5878–5888.
[58] P.R. da Silva, M.D.C.A. de Lima, T.P. Souza, J.M. Sandes, A.D.C.A. de Lima, P.J. R. Neto, F.A.B. Dos Santos, L.C. Alves, R.M.F. da Silva, G.J. de Moraes Rocha, I. J. da Cruz Filho, Lignin from *Morinda citrifolia* leaves: Physical and chemical characterization, in vitro evaluation of antioxidant, cytotoxic, antiparasitic and ultrastructural activities, Int. J. Biol. Macromol. 193 (2021) 1799–1812.
[59] O. Gordobil, R. Herrera, M. Yahyaoui, S. İlk, M. Kaya, J. Labidi, Potential use of kraft and organosolv lignins as a natural additive for healthcare products, RSC Adv. 8 (43) (2018) 24525–24533.
[60] C. Chio, M. Sain, W. Qin, Lignin utilization: a review of lignin depolymerization from various aspects, Renew. Sustain. Energy Rev. 107 (2019) 232–249.
[61] J. Dominguez-Robles, E. Larraneta, M.L. Fong, N.K. Martin, N.J. Irwin, P. Mutje, Q. Tarres, M. Delgado-Aguilar, Lignin/poly(butylene succinate) composites with antioxidant and antibacterial properties for potential biomedical applications, Int. J. Biol. Macromol. 145 (2020) 92–99.
[62] K.R. Aadil, D. Prajapati, H. Jha, Improvement of physio-chemical and functional properties of alginate film by Acacia lignin, Food Pack. Shelf, Life 10 (2016) 25–33.
[63] E. Lee, Y. Song, S. Lee, Crosslinking of lignin/poly(vinyl alcohol) nanocomposite fiber webs and their antimicrobial and ultraviolet-protective properties, Text. Res. J. 89 (1) (2019) 3–12.